Synthesis and Characterization of PMMA-Cellulose Nanocomposites by *In Situ* Polymerization Technique

Sunanda Sain,[1] Dipa Ray,[1] Anirudhha Mukhopadhyay,[2] Suparna Sengupta,[3] Tanusree Kar,[4] Christopher J. Ennis,[5] Pattanathu K. S. M. Rahman[5]

[1]*Department of Polymer Science & Technology, University of Calcutta, Kolkata 700009, India*
[2]*Department of Environmental Science, University of Calcutta, Kolkata 700019, India*
[3]*Calcutta Institute of Engineering & Management, Tollygunge, Kolkata 700040, India*
[4]*Department of Materials Science, Indian Association for the Cultivation of Science, Kolkata 700032, India*
[5]*School of Science and Engineering, Teesside University, Middlesbrough TS13BA, United Kingdom*

Received 12 January 2011; accepted 27 December 2011
DOI 10.1002/app.36723
Published online in Wiley Online Library (wileyonlinelibrary.com).

ABSTRACT: Cellulose nanoparticles (CNPs) were prepared from jute fiber by acid hydrolysis followed by high-speed homogenization. The CNPs were used as fillers in the production of polymethylmethacrylate (PMMA) nanocomposites by *in situ* suspension polymerization technique. The suspension polymerization of MMA was carried out in the presence of CNPs, which were dispersed in water medium and *in situ* PMMA/cellulose nanocomposite granules were formed. PMMA polymer, without any filler, was also prepared by similar suspension polymerization technique. PMMA and PMMA/cellulose nanocomposite films were prepared by solution casting method. Viscosity average molecular weights of neat PMMA and the PMMA extracted from PMMA/cellulose nanocomposite granules were determined by viscometric method and average molecular mass of PMMA extracted from PMMA/cellulose nanocomposites was found to be reduced than that of neat PMMA. Attenuated total reflectance Fourier transform infrared spectroscopy was performed to find out any chemical interaction between polymer matrix and the CNPs. X-ray diffraction study and differential scanning calorimetry were done to investigate the structures of the nanocomposite films and the glass transition temperature was found to be lower in the nanocomposite than that in the virgin polymer. Field emission scanning electron microscopy and atomic force microscopy were done to examine the morphology of the films. Such an *in situ* suspension polymerization technique for the preparation of PMMA/cellulose nanocomposites can be very useful to prepare tailor-made materials. © 2012 Wiley Periodicals, Inc. J Appl Polym Sci 000: 000–000, 2012

Key words: nanocomposites; thermoplastics; atomic force microscopy; differential scanning calorimetry

INTRODUCTION

Nanocomposite describes a two-phase material where one of the phases has at least one dimension in nanometer range (1–100 nm). The attractiveness of polymer-nanocomposites resides in the potential of adding nanometer-sized small fillers such as different types of nanoclay and so on, to dramatically raise the mechanical, thermal, barrier, and flame-retardant properties, without increasing the specific gravity or reducing the transparency of the nanocomposites relative to the base material.[1–4] Recently, significant attention has been given toward the development and investigation of polymer nanocomposites with the expectation that this can lead to lighter and better materials for engineering applications.[5–7]

Poly(methyl methacrylate) (PMMA) is one of the promising polymeric materials in this respect, with several desirable properties including good weatherability, high strength, excellent optical clarity, and dimensional stability. Most of the previous work on this system has been done on PMMA-inorganic filler nanocomposites.[8,9]

In order to reduce the environmental pollution caused by polymers, attempts are being made to modify their structures by blending or combining them with other biodegradable materials.[10,11] Hence, the combination of polymers with cellulosic materials as, for example, blends, composites, nanocomposites and so on, are important areas of current research.

There are very few reports of PMMA-cellulose nanocomposite formation by *in situ* polymerization technique.[12] Mabrouk et al. used one-step method to prepare stable aqueous nanocomposite dispersions based on cellulose whiskers and acrylate latex via mini emulsion polymerization. Nanocomposites

Correspondence to: D. Ray (roy.dipa@gmail.com).
Contract grant sponsors: University Grants Commission (UGC), Government of India.

materials were prepared from these dispersions using a casting/evaporation method. They studied thermal and mechanical properties of the nanocomposites using differential scanning calorimetry (DSC) and dynamic mechanical analysis.[12] There are some reports on *ex situ* PMMA-cellulose nanocomposite formation. Liu et al.[13] fabricated nano-sized cellulose particles from microcrystalline cellulose (MCC), which were then utilized to prepare PMMA nanocomposites by solution casting method. Besides, these there are some works reported on PMMA-cellulose blend[14] and acrylic resin-bacterial cellulose nanocomposites.[15,16]

Our objective in this work was to develop PMMA/cellulose nanocomposites through *in situ* polymerization and to make a comparative study of the structures of PMMA and PMMA/cellulose nanocomposites. The structures were investigated with attenuated total reflectance Fourier transform infrared spectroscopy (ATR-FTIR), X-ray diffraction (XRD), DSC, and TGA. The surface morphologies were examined by field emission scanning electron microscopy (FE-SEM) and atomic force microscopy (AFM).

EXPERIMENTAL

Materials

Methyl methacrylate monomer used in this study was procured from Merck, Germany. Benzoyl peroxide (BP) and polyvinyl alcohol (PVOH), sodium chlorite, and sodium bisulfite (used for delignification step) were supplied by Loba Chemie, Mumbai. Cellulose was extracted from raw jute. Sodium hydroxide (NaOH) and acetic acid, obtained from Merck, were used for removal of hemicellulose fraction from jute fibers. Sulfuric acid (Merck Product) was used for acid hydrolysis. A high speed homogenizer (Remi High Speed Homogenizer Model No. RQ 127A) was used to reduce the cellulose particle size to nanolevel.

Preparation of the cellulose nanoparticles

A total of 1 g raw jute was treated with 50 mL of 0.7% sodium chlorite ($NaClO_2$) solution at pH = 4 and kept for 2 h at near boiling temperature with continuous stirring to remove the lignin and hemicellulose fraction.[17] The treated mass was filtered, washed with distilled water, and put into 2% sodium bisulfite solution for 15 min. It was then filtered, washed with distilled water, and dried in an oven until constant weight was reached. This dried mass was then treated with 17.5% NaOH solution for 15 min and macerated to remove the hemicellulose fraction. Finally, this chemically treated mass was filtered, washed with distilled water to remove the alkali, and subjected to acid hydrolysis (47% sulfuric acid) with constant stirring for 3 h at 50°C following the standard hydrolysis procedure of Dong et al.[18] The prepared cellulose nanoparticles (CNPs) were washed with distilled water and centrifuged several times to remove the acid, and the concentrated mass was freeze dried at −20°C at a pressure of 15 Pa using Eyela Freeze Drier FD-5N, Japan, when dry nanocellulose powder was obtained.

Preparation of the PMMA/cellulose nanocomposites by *in situ* suspension polymerization

CNPs, 0.3% w/w with respect to the monomer, were dispersed in deionized water. PVOH (6% w/v with respect to the monomer), the suspension stabilizer, was added to water and heated to 85°C. Benzoyl peroxide (3% w/v), the free radical initiator, was added to the monomer MMA. The mixture of MMA and benzoyl peroxide was then slowly added into the suspension medium in the reactor. The reaction was carried out at 85°C for 4 h and then at 90°C for 1 h with continuous stirring with a mechanical stirrer [Remi mechanical stirrer-Universal Motor, Type- RQ-122, Remi Motors, Vasai-401208 (India)] maintaining a rotation speed 3000 rpm. PMMA/cellulose nanocomposite granules were formed in the suspension medium. The granules were filtered, rinsed with hot water several times to remove PVOH, and dried under vacuum at 80°C overnight. Pure PMMA, without any filler, was also prepared by the same suspension polymerization technique.

Preparation of the PMMA and PMMA/cellulose nanocomposite film

PMMA and PMMA/cellulose nanocomposite films were prepared by solution casting method. PMMA and PMMA/cellulose nanocomposite granules were dissolved in chloroform separately to form a 2% (w/v) solution and sonicated for 3 h. The solutions were then cast on two separate Petri dishes to prepare solution cast films. The films were dried at room temperature followed by drying in a hot air oven for 30 min at 50°C.

Characterizations of polymer and polymer nanocomposite

Particle size analysis was done to characterize the CNPs with Malvern V2.0 (Malvern Instruments), and size distribution was reported by intensity. Average diameter of the prepared CNPs was in 458 nm range.

The viscosity average molecular weight ($\overline{M}_v$) of the neat PMMA and PMMA extracted from PMMA/cellulose nanocomposite was determined by

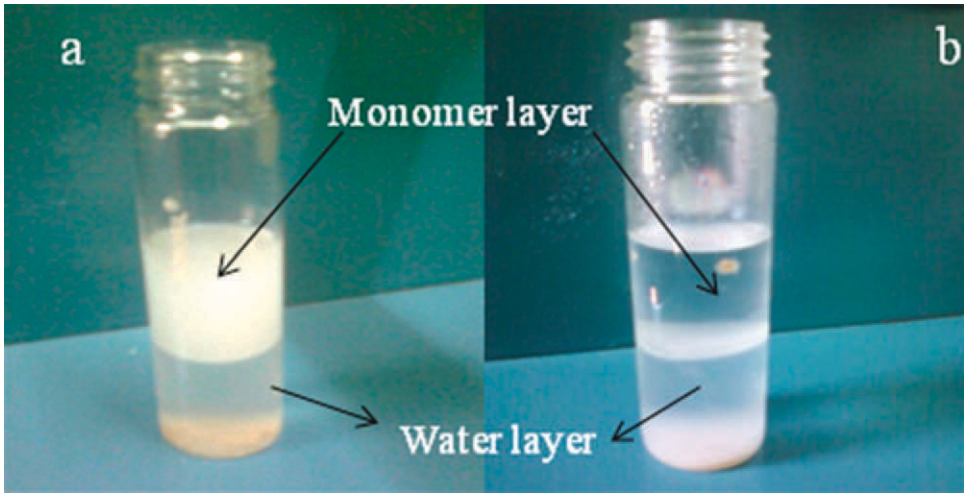

Figure 1 (a) Dispersion of cellulose nanoparticles into water and MMA just after sonication. (b) Dispersion of cellulose nanoparticles into water and MMA after 5 min of the sonication. [Color figure can be viewed in the online issue, which is available at wileyonlinelibrary.com.]

viscometric method in chloroform, following the Mark-Houwink equation: $[\eta] = K\overline{M}_v{}^{\alpha}$, where $[\eta]$ is the intrinsic viscosity of the solution, $K = 0.34 \times 10^{-4}$ (Ref. [19]) and $\alpha = 0.83$ at 25°C for chloroform. The unit of Mark-Houwink intercept is inverse concentration, that is, dL/gm.

ATR-FTIR spectra of the pure PMMA and PMMA-cellulose nanocomposite powder and film were recorded on a Perkin-Elmer infrared spectrometer (Spectrum RX 73713 series) equipped with a single reflection diamond ATR accessory. Sample data were ratioed against background spectra obtained from the clean crystal. A force of 40 N was applied to the ATR crystal for all spectra and the spectra were corrected using the on-board Perkin-Elmer ATR correction algorithm.

X-ray diffraction patterns were obtained by using an X-ray diffractometer (X'Pert PRO) Model RIGAKU MINISLEX with a nickel-filtered Cu Kα line ($\lambda = 0.15404$ nm), operated at 40 kV × 100 mA and a scanning rate of 2° min^{-1}. Scans were taken in the range of diffraction angle $2\theta = 0$–60°.

The thermal transitions of PMMA and PMMA/cellulose nanocomposites were determined with the DSC (DSC Q20 V24.4 Build 116, TA Instruments). Samples were heated from room temperature to 250°C, cooled from 250°C to room temperature, and then reheated from room temperature to 250°C, and each cycle was carried out at a rate of 10°C min^{-1} in nitrogen atmosphere.

Thermal stability of the samples was studied with thermogravimetric analysis (TGA Q50 V20.10 Build 36) from room temperature to 600°C at a rate of 10°C min^{-1} in nitrogen atmosphere.

Surface morphology of the PMMA and PMMA/cellulose nanocomposite powder was studied by scanning electron microscope (HITACHI-S-3400N) and a field emission scanning electron microscope (Model-JEOL JEM-6700F) was used to study the surface morphology of the PMMA film and PMMA/cellulose nanocomposite film. All the samples were coated with a thin layer of gold prior to testing.

The surface morphology of the pure PMMA and the PMMA/cellulose nanocomposite films were also analyzed with a Veeco MultiMode scanning probe microscope with a Nanoscope IIIa controller. Images were collected using a tapping mode having a phosphorous-doped silicon tip (Model no. RTESP) with a nominal frequency of 312 kHz.

RESULTS AND DISCUSSION

In this work, PMMA/cellulose nanocomposite was prepared by *in situ* suspension polymerization technique. The CNPs had an average particle size around 457 nm. Before preparing PMMA and PMMA/cellulose nanocomposite granules, a simple experiment was done to determine the dispersibility of CNPs in MMA in comparison to water.[20] A measured amount of CNPs was first dispersed in 5 mL of water by sonication. Then, 5 mL of MMA was added to the water-cellulose suspension and sonicated for 30 min. The weight of cellulose was 0.3% with respect to the weight of MMA taken. After sonication, the water-MMA-cellulose mix was immediately poured in a glass bottle [Fig. 1(a)]. It was clearly visible that a part of the CNPs was uniformly dispersed in MMA (upper layer), while the remaining amount settled immediately at the bottom of the water layer (lower layer). The water layer appeared clearer and the amount of cellulose settled at the bottom was measured, and the cellulose dispersed in the MMA phase was calculated to be nearly 6%

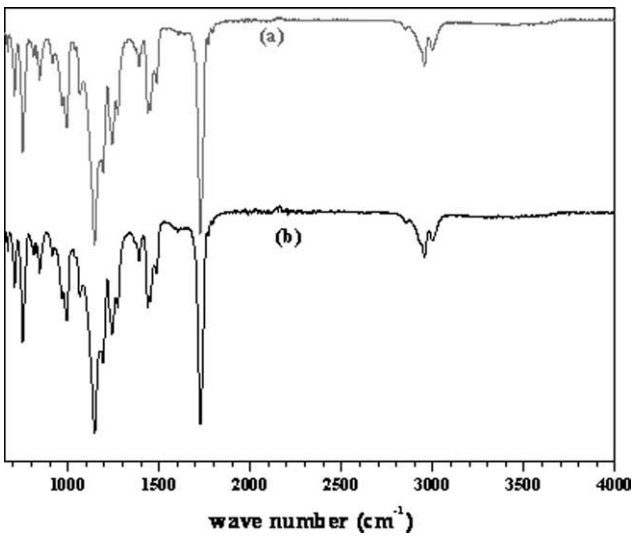

Figure 2 ATR-FTIR spectra of: (a) pure PMMA film; (b) PMMA/cellulose nanocomposite film.

of the total weight of cellulose taken. After standing for 5 min, the cellulose dispersed in the MMA phase started to accumulate at the MMA-water interface [Fig. 1(b)]. This observation gave a strong indication that a small amount of the CNPs will remain in intimate contact with the MMA monomer during the suspension polymerization and they might get embedded within the polymer molecules during long chain formation and influences the polymerization process. In addition, the major part of cellulose will remain dispersed in water due to continuous stirring and will remain present in the medium during PMMA molecule formation.

Characterization/identification

Molecular weight determination by viscometric method

The viscosity average molecular weight of PMMA and PMMA extracted from the *in situ* PMMA/cellulose nanocomposite film was determined by viscometric method. The viscosity average molecular weight ($\overline{M}_v$) of PMMA extracted from the PMMA/cellulose nanocomposite was 49,964 g/mol, whereas for pure PMMA, it was 56,726 g/mol. The decrease in molecular weight value of PMMA in presence of CNPs might be due to the plasticizing effect of the nanofiller. The presence of CNPs during polymerization might affect the polymerization kinetics and mechanism that reduced the molecular weight.[19,21]

Attenuated total reflectance Fourier transform infrared spectroscopy

No significant differences were observed between the normalized ATR-FTIR spectra of pure PMMA and PMMA-cellulose nanocomposite film (Fig. 2). The major features of the pure PMMA spectra are: the α-methyl, ester-methyl, and methylene C—H stretching (3100–2800 cm^{-1}) and bending (1500–1350 cm^{-1}) modes[22,23]; the C=O stretching mode (1728 cm^{-1})[22,23]; and three bands in the 1350–1100 cm^{-1} region of the spectrum, which have been assigned to ester group stretching vibrations[22,24] or the coupled C—O and antisymmetric C—C—O stretch (1242 cm^{-1}) and skeletal vibrations coupled to C—H deformations (1194 and 1150 cm^{-1}).[25] The band at 843 cm^{-1} is assigned to the methylene rocking mode,[24] whereas the latter two bands at 827 and 809 cm^{-1} are associated with vibrations of the ester group,[24] possibly the C—O—C symmetric stretching mode.[24] These were all observed to be unaltered by the presence of CNPs. Thus, no chemical interaction or chemical bond formation was evident during the *in situ* polymerization of MMA monomer in presence of CNPs.

XRD spectra

X-ray diffraction spectra of the prepared CNPs, PMMA, and PMMA/cellulose nanocomposite films are shown in Figure 3. It was seen in our previous article[26] that in case of raw jute fiber a broad peak appeared around 15.8° (due to the presence of cellulose I) and a distinct peak appeared at $2\theta = 22.48°$, which are the characteristics of cellulose I. These peaks diminished significantly in case of our prepared CNPs.[26] Instead, a very sharp peak appeared at 20°, which can be attributed to the (101) plane of cellulose II. This observation indicated that the cellulose I structures were significantly reduced in the prepared CNPs due to the various chemical treatments followed by acid hydrolysis and

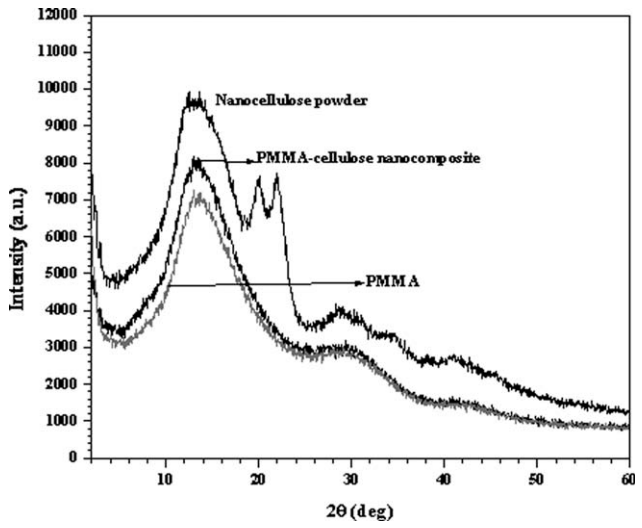

Figure 3 XRD spectra of prepared nanocellulose, PMMA and PMMA/cellulose nanocomposite films.

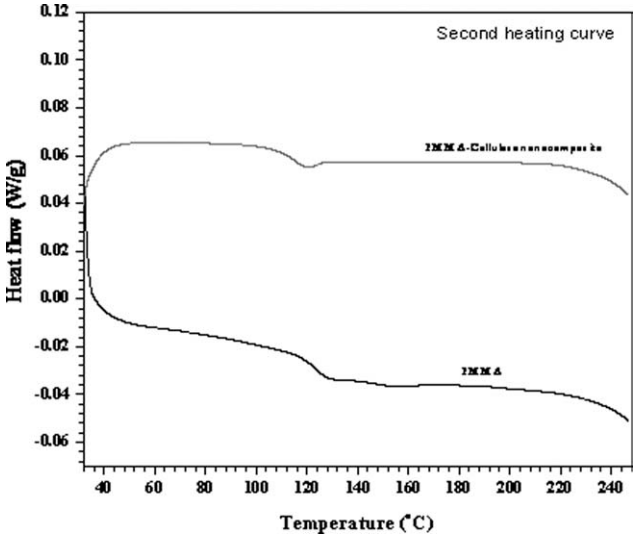

Figure 4 DSC second heating curves of PMMA and PMMA/cellulose nanocomposite films.

consequently, cellulose-II structures became prevalent.[27] PMMA showed one large diffraction maxima at $2\theta = 13.4°$ and a small hump at 30.2°, indicating the ordered packing of the polymer chains and the effect of ordering inside the main chains, respectively.[22] The presence of broad humps, that is, absence of any prominent peak in the XRD spectrum confirmed the predominantly amorphous nature of the PMMA film. The absence of any sharp peak in case of PMMA-cellulose nanocomposite indicated that addition of this small amount of CNPs did not impose any crystallinity in the structure of the polymer matrix.[22,28]

Thermal analysis

Differential scanning calorimetry

Figure 4 illustrates the DSC pattern of PMMA and PMMA/cellulose nanocomposite films. In the second heating curve (Fig. 4), T_g was observed at 123°C for PMMA, while, in PMMA/cellulose nanocomposites, T_g shifted to 115°C. This shift of T_g to a lower temperature in PMMA/cellulose nanocomposites indicated that the presence of such small amount of cellulose particles (0.3 wt %) facilitated the overall segmental mobility of the PMMA chains at a lower temperature.[13] These results suggest that the cellulose particles significantly influenced the molecular rearrangement process during phase transition. DSC result supports the viscosity average molecular weight result also.

TGA

Figure 5(a,b) shows the TG and DTG curves, respectively, of pure PMMA and PMMA/cellulose nanocomposite. The DTG curve of PMMA showed four distinct peaks at around 165, 263, 286, and 370°C. PMMA/cellulose nanocomposite showed a sharp peak around 377°C and four other small peaks at around 146, 175, 240, and 286°C. The peak ranging from 165–195°C corresponded to the cleavage of the carbon–carbon bonds between units linked head to head. The peaks ranging from 270–300°C corresponded to the cleavage of terminal vinyl units, and the highest peak may be caused by random scission initiation and here intense weight loss occurred owing to the cleavage of the most stable bonds between units linked head-to-tail.[29] The lower decomposition peak (at around 146°C) in PMMA/cellulose nanocomposite might have resulted from the decomposition of cellulose fraction.[30] The nanocomposite began to degrade at a comparatively lower temperature than that of pure PMMA. Table I

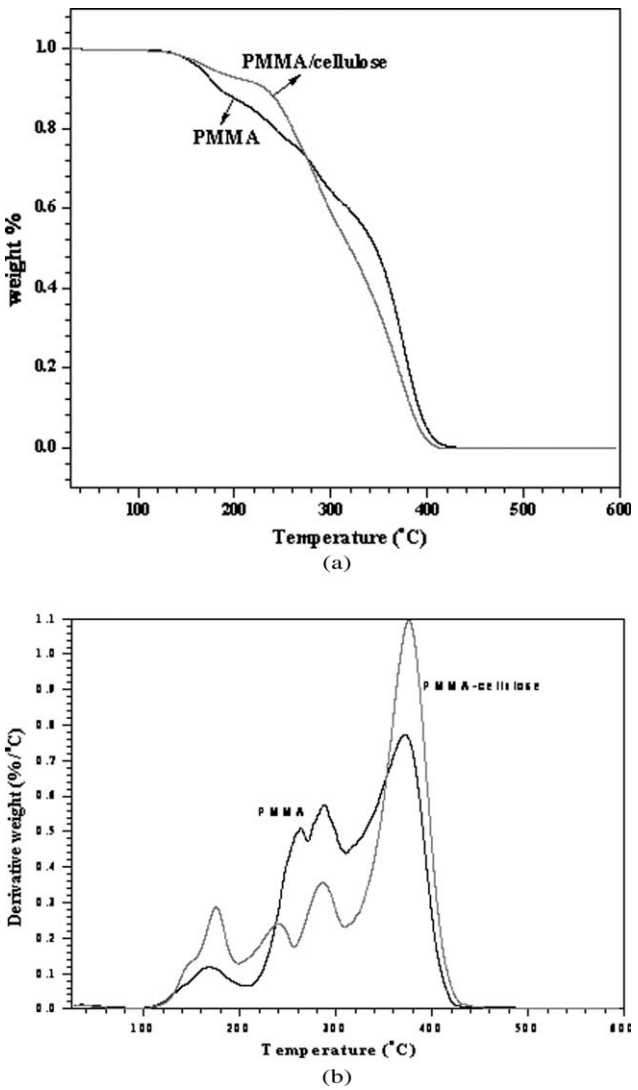

Figure 5 (a) TGA curves of PMMA and PMMA/cellulose nanocomposite films; (b) DTG curves of PMMA and PMMA/Cellulose nanocomposite films.

TABLE I
TGA Results of Suspension-Polymerized PMMA and Its Nanocomposite with 0.3 wt % Cellulose Loading

Sample details	T_I (°C)	T_{50} (°C)	T_{max}(°C)	Weight % loss (max.)
PMMA	165	346	412	99.98
PMMA/cellulose nanocomposite	146	320	403	99.9

shows the initial degradation temperature (T_I), the temperature corresponding to the 50% weight loss (T_{50}), and maximum degradation temperature (T_{max}) of neat PMMA and PMMA/cellulose nanocomposite. The decomposition peak shifted to a significantly lower temperature in the nanocomposite than that observed for pure PMMA, which could be due to the incorporation of the cellulose nanofiller, which affected the entanglement of the polymer chains.

The main degradation peak appeared at 370°C in PMMA, while it shifted to 377°C in PMMA-cellulose nanocomposites. However, the rate of degradation was higher in PMMA-cellulose nanocomposites than that observed in PMMA. This implies that the presence of CNPs encapsulated within the PMMA chains might have delayed the onset of thermal degradation which shifted to a higher temperature of 377°C, but once degradation started, the rate became very high because cellulose itself also degrades at this temperature.

Microscopic analysis

SEM analysis

Figure 6(a,b) represents the SEM micrograph of PMMA and PMMA/cellulose nanocomposite beads, respectively, prepared by suspension polymerization. The PMMA particles were found to be of various sizes ranging between 10–80 μm and the size distribution was not uniform. The bead size increased considerably (∼ 150 μm) in case of PMMA/cellulose nanocomposite. It was apparent from the SEM micrograph of PMMA/cellulose nanocomposite beads [Fig. 6(b)] that some cellulose particles might have reaggregated among themselves and adhered to the polymer surface. During the reaction, the hydrophilic CNPs migrated to the polymer water interface, which might be due to either Van der Waal's attraction[22] or due to strong hydrogen bonding interaction among themselves and the distribution was not uniform. Agglomeration also occurred due to the incompatibility between the hydrophilic cellulose surface and hydrophobic nature of the polymer molecules.

Figure 7(a,b) show the FE-SEM images of the surfaces of PMMA and PMMA/cellulose nanocomposite films. In PMMA film, very few partially dissolved granules were observed.[31] In PMMA/

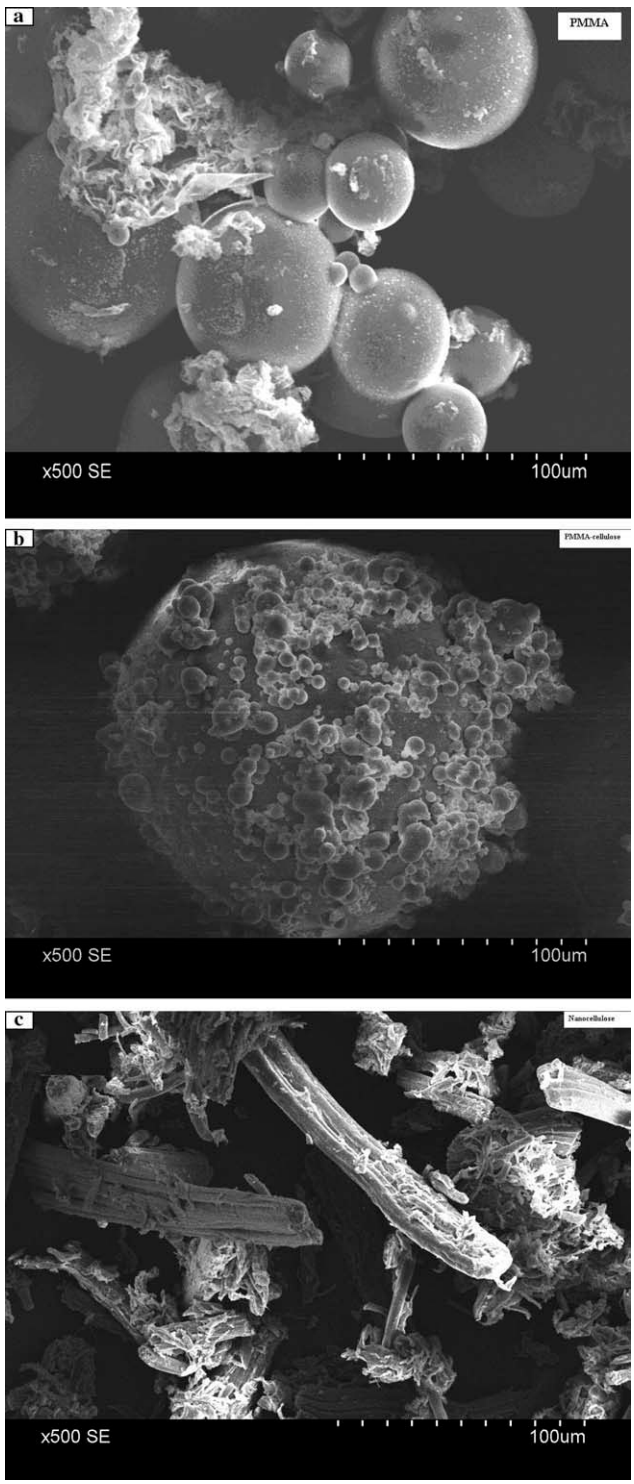

Figure 6 SEM images of (a) PMMA, (b) PMMA/cellulose nanocomposite powder, and (c) nanocellulose powder.

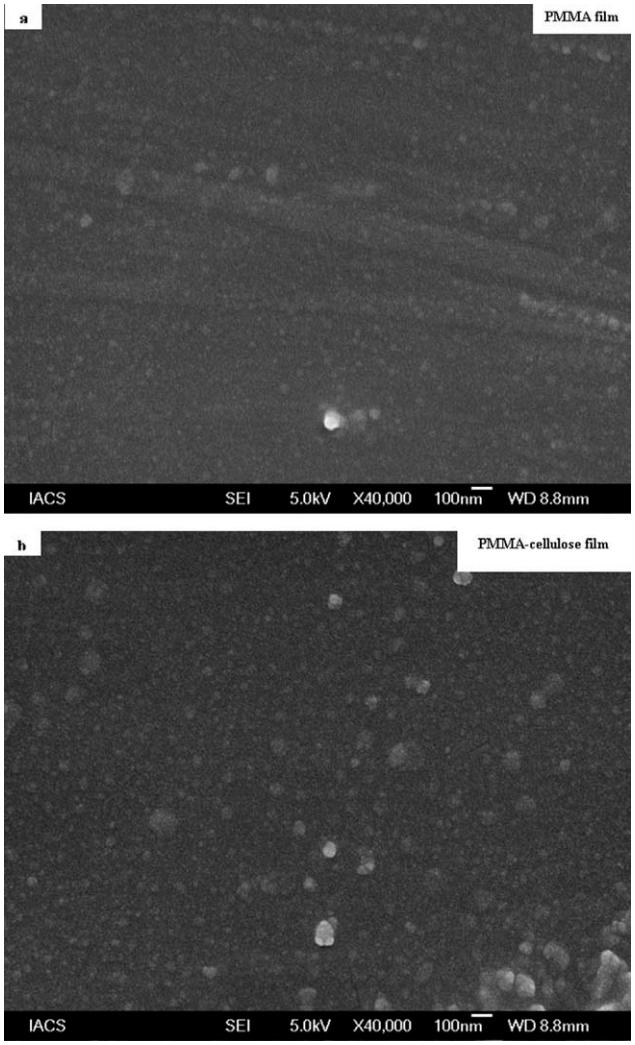

Figure 7 FE-SEM images of (a) PMMA and (b) PMMA/cellulose nanocomposite films.

cellulose film, CNPs were seen to be uniformly dispersed in the PMMA matrix along with some partially dissolved PMMA/cellulose granules. The dispersed particles had diameters below 100 nm, which also gave an idea about the size of the prepared CNPs.

AFM analysis

Figure 8(a–c) represents the AFM surface images of CNPs, pure PMMA, and PMMA/cellulose nanocomposite film, respectively. The AFM image of CNPs in Figure 8(a) revealed a triangular pattern. The AFM images of the surface of the films showed that both the surfaces of the neat polymer and the nanocomposite film were not homogeneous and surface roughness increased when CNPs were present in the PMMA matrix.[32] Figure 8(b) showed some aggregates, which might be due to the undissolved PMMA particles during film preparation. The height image barely showed the valleys and hills of the surface corresponding to the dark and bright regions. The effect of CNP addition on the nanocomposite structure was distinctly visible in Figure 8(c), which indicated the formation of up and down regions similar to that observed for CNPs.[27] A large number

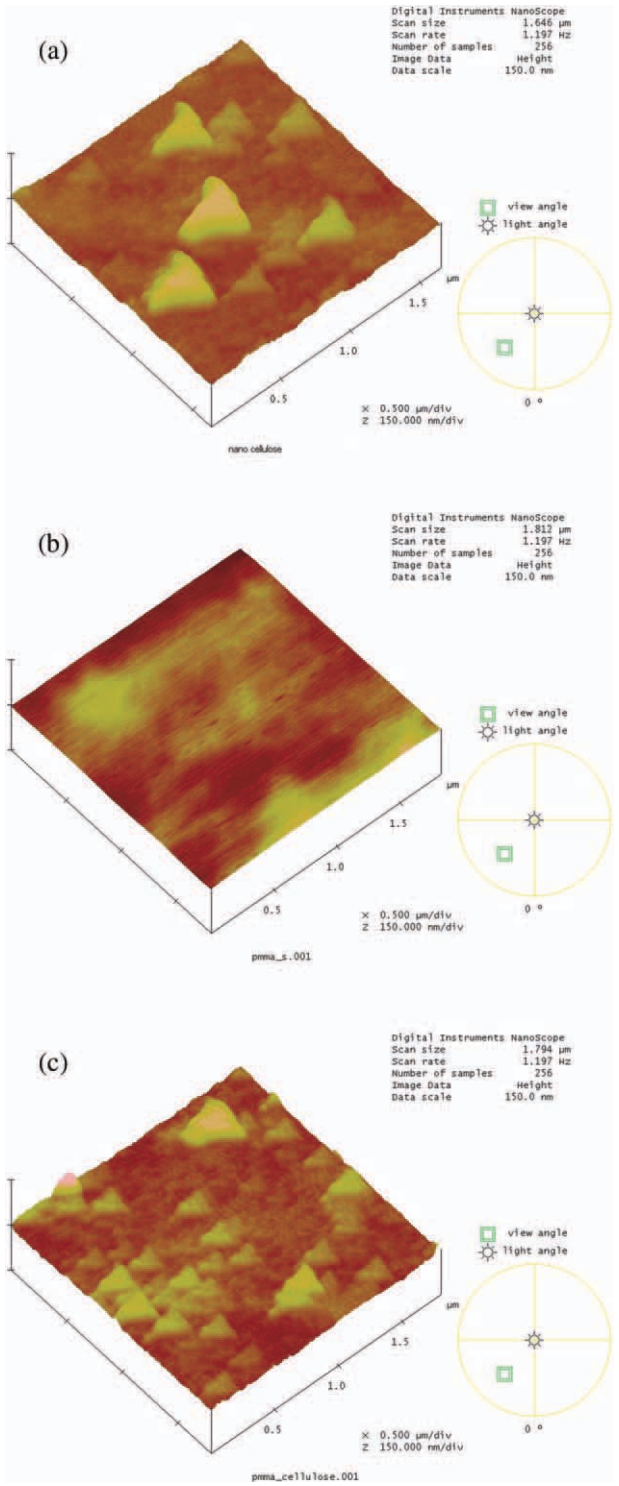

Figure 8 3D views of AFM images of (a) cellulose nanoparticles, (b) PMMA, and (c) PMMA/cellulose nanocomposite films. [Color figure can be viewed in the online issue, which is available at wileyonlinelibrary.com.]

of bright areas in both the height and phase images indicated the presence of CNPs.[33]

CONCLUSIONS

CNPs were prepared from jute fiber using sulfuric acid-hydrolysis method combined with high-speed homogenization. PMMA/cellulose nanocomposite granules were successfully prepared by *in situ* suspension polymerization technique. PMMA/cellulose nanocomposite films were prepared by solution casting method. The presence of small amount of CNPs in PMMA/cellulose nanocomposites facilitated the overall segmental mobility of the PMMA molecules and the T_g shifted to a lower temperature in PMMA/cellulose nanocomposites than that observed for PMMA alone. The CNPs present in the PMMA matrix increased the onset of degradation temperature, shifted the peak degradation to a higher temperature but the rate of degradation also increased significantly. These results indicate that *in situ* suspension polymerization technique can be utilized effectively to prepare PMMA-cellulose nanocomposites with tailored properties.

References

1. Kim, Y. K.; Choi, Y. S.; Wang, K. H.; Chung, I. J. Chem Mater 2002, 14, 4990.
2. Wang, D.; Zhu, J.; Yao, Q.; Wilkie, C. A. Chem Mater 2002, 14, 3837.
3. Fu, X.; Qutubuddin, S. Polymer 2001, 42, 807.
4. Okamoto, M.; Morita, S.; Kim, Y. H.; Kotaka, T.; Tateyama, H. Polymer 2001, 42, 1201.
5. Zeng, C.; Lee, L. J. Macromolecules 2001, 34, 4098.
6. Manias, E.; Touny, A.; Wu, L.; Strahecker, K.; Lu, B.; Chung, T. C. Chem Mater 2001, 13, 3516.
7. Choi, Y. S.; Wang, K. H.; Xu, M.; Chung, I. J. Chem Mater 2002, 14, 2936.
8. Kimy, S.; Wilkie, C. A. Polym Adv Technol 2008, 19, 496.
9. Kulyk, B.; Kapustianyk, V.; Tsybulskyy, V.; Krupka, O.; Sahraoui, B. J Alloys Compds 2010, 502, 24.
10. Albertson, A. C.; Ljungquist, O. Acta Polym 1998, 39, 95.
11. Tudorachi, N.; Cascaval, C. N.; Rusu, M. J Polym Eng 2000, 20, 287.
12. Mabrouk, A. B.; Kaddami, H.; Magnin, A.; Belgacem, M. N.; Dufresne, A.; Boufi, S. Polym Eng Sci 2011, 51, 62.
13. Liu, H.; Liu, D.; Yao, F.; Wu, Q. Bioresour Technol 2010, 101, 5685.
14. Bhat, K. D.; Kumar, S. M. J Polym Environ 2006, 14, 385.
15. Ifuku, S.; Nogi, M.; Abe, K.; Handa, K.; Nakatsubo, F.; Yano, H. Biomacromolecules 2007, 8, 1973.
16. Nogi, M.; Abe, K.; Handa, K.; Nakatsubo, F.; Ifuku, S.; Yano, H. Appl Phys Lett 2006, 89, 233123.
17. Purkait, B. S.; Ray, D.; Sengupta, S. Ind Eng Chem Res 2011, 51, 62.
18. Dong, X. M.; Revol, J. F.; Gray, D. G. Cellulose 1998, 5, 19.
19. Khatana, S.; Dhibar, A. K.; Ray, S. S.; Khatua, B. B. Macromol Chem Phys 2009, 210, 1104.
20. Khaled, S. M.; Sui, R.; Charpentier, P. A.; Rizkalla, A. S. Langmuir 2007, 23, 3988.
21. Liqiang, C.; Naresh, T. N. H.; Ihl, W. S. Macromolecules 2008, 41, 4268.
22. Ahmad, S.; Ahmad, S.; Agnihotry, S. A. Bull Mater Sci 2007, 30, 31.
23. Pandey, J. K.; Chu, W. S.; Kim, C. S.; Lee, C. S.; Ahn, S. H. Composites: Part B 2009, 40, 676.
24. Na, M.; Rhee, S. W. Org Electron 2006, 7, 205.
25. Lu, P.; Hsieh, Y. L. Nanotechnology 2009, 20, 415604 (9pp).
26. Siqueira, G.; Bras, J.; Dufresne, A. Langmuir 2010, 26, 402.
27. Das, K.; Ray, D.; Banerjee, C.; Bandyopadhyay, N. R.; Sahoo, S.; Mohanty, A. K.; Misra, M. Ind Eng Chem Res 2010, 49, 2775.
28. Enomoto-Rogers, Y.; Kamitakahara, H.; Takano, T.; Nakatsubo, F. Biomacromolecules 2009, 10, 2110.
29. Kashiwagi, T.; Inaba, A.; Brown, J. E.; Hatada, K.; Kitayama, T.; Masuda, E. Macromolecules 1986, 19, 2160.
30. Nishioka, N.; Yamaoka, M.; Haneda, H.; Kawakami, K.; Uno, M. Macromolecules 1993, 26, 4694.
31. Verma, H. K.; Sreenivasan, K.; Yokogawa, Y.; Hosumi, A. Biomaterials 2003, 24, 297.
32. Lewis, S.; Haynes, V.; Wheeler-Jones, R.; Sly, J.; Perks, R. M.; Piccirillo, L. Thin Solid Films 2010, 518, 2683.
33. Liu, W.; Wu, L.; Tian, X.; Zheng, J.; Cui, P.; He, S.; Zhu, C. Polym Bull 2010, 65, 133.